

Robust Ionic Current Sensor for Bacterial Cell Size Detection

Hirotohi Yasaki,^{*,†,‡,§} Taisuke Shimada,^{†,‡} Takao Yasui,^{†,‡,§} Takeshi Yanagida,^{||,⊥} Noritada Kaji,^{†,‡,§} Masaki Kanai,^{||} Kazuki Nagashima,^{||} Tomoji Kawai,[⊥] and Yoshinobu Baba^{*,†,‡,§}

[†]Department of Biomolecular Engineering, Graduate School of Engineering and [‡]ImPACT Research Center for Advanced Nanobiodevices, Nagoya University, Furo-cho, Chikusa-ku, Nagoya 464-8603, Japan

[§]Japan Science and Technology Agency (JST), PRESTO, 4-1-8 Honcho, Kawaguchi, Saitama, 332-0012, Japan

^{||}Laboratory of Integrated Nanostructure Materials Institute of Materials Chemistry and Engineering, Kyushu University, 6-1 Kasuga-koen, Kasuga, Fukuoka 816-8580, Japan

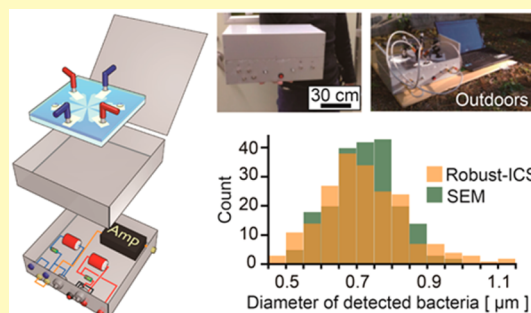
[⊥]Institute of Scientific and Industrial Research, Osaka University, Mihogaoka, Ibaraki 567-0047, Osaka, Japan

[#]Health Research Institute, National Institute of Advanced Industrial Science and Technology (AIST), Takamatsu 761-0395, Japan

Supporting Information

ABSTRACT: Ionic current sensing methods are useful tools for detecting sub- to several-micron scale particles such as bacteria. However, conventional commercially available ionic current sensing devices are not suitable for on-site measurement use because of inherent limitations on their robustness. Here, we proposed a portable robust ionic current sensor (Robust-ICS) using a bridge circuit that offers a high signal-to-noise (S/N) ratio by suppressing background current. Because the Robust-ICS can tolerate increased noise in current sensing, a simple, lightweight electromagnetic shield can be used and measurements under large electromagnetic noise conditions can be made. The weight of the device was lowered below 4 kg and outdoor particle detection measurements were completed successfully. Accuracy of size detection of *Staphylococcus aureus* (*S. aureus*) was equivalent to that obtained by SEM imaging.

KEYWORDS: ionic current sensing, bridge circuit, micropore, robust sensor, bacteria



Bacteria are known to cause food poisoning^{1–4} and infectious diseases.^{5,6} The incubation period of food poisoning by *Staphylococcus aureus* (*S. aureus*) has been reported to be 2–6 h.⁷ Being able to identify causative bacteria using on-site rapid detection methods would help to prevent the spread of food poisoning and infectious diseases by such quickly incubating bacteria. Ionic current sensing methods have attracted attention as detection methods for various sub- to several-micron-sized harmful particles, including bacteria.⁸ In ionic current sensing, a voltage is applied to a micropore filled with conductive solution and the current flow change by passing of a sample particle is monitored.⁹ This current change is defined as a signal. Bacteria species having various indigenous sizes can be discriminated based on the amplitude of the signals corresponding to cell volume; e.g., *S. aureus* has a volume of about 0.4 fL and *Bacillus subtilis* (*B. subtilis*) has a volume of 1.5 to 4.2 fL.^{10,11}

However, the conventional ionic current sensing methods have only been reported for detections in a controlled environment such as a laboratory,^{12–15} and particle detections in an uncontrolled environment such as outdoors have not been demonstrated. The reason is that it is necessary to lower the electromagnetic noise to detect a small-sized sample particle because of the inherently poor signal-to-noise (S/N) ratio of the conventional methods. Consequently, in many commer-

cially available devices,^{14,16} a thick electromagnetic shield is used to lower noise from outside the device, and portability is impaired. To the best of our knowledge, qNano,¹⁷ which is the particle detector presently offering the highest portability, has only been used in a controlled laboratory environment. Therefore, for conventional methods, it is necessary to transport samples to a laboratory, and it remains difficult to detect the bacteria on-site.

In order to enable rapid bacteria detection anywhere, we developed a robust ionic current sensor (Robust-ICS) with a bridge circuit. Although the bridge circuit is a classical electric circuit, the combination of the bridge circuit and ionic current sensing enhanced the S/N ratio by suppressing the background current, and small particle detection in a large electromagnetic noise environment became possible.¹⁸ We fabricated the Robust-ICS by superimposing a detection unit, using a microfluidic chip, and an electric circuit unit, covered with an aluminum plate shield to lower the device weight (Figure 1a). In this paper, we show that ionic current sensing using our

Received: January 15, 2018

Accepted: February 8, 2018

Published: February 8, 2018

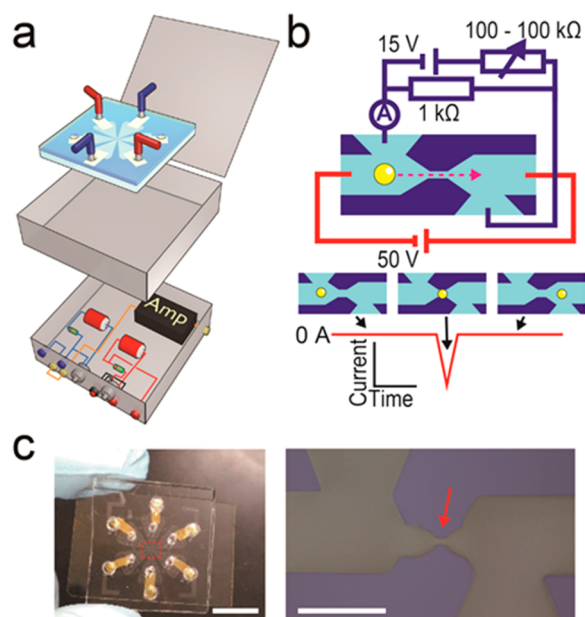


Figure 1. Schematic illustration of the robust ionic current sensor and photo images of the micropore chip. (a) Conceptual illustration of the robust ionic current sensor (Robust-ICS). Upper and lower boxes are detection and electric circuit units, respectively. (b) Detection mechanism of current signals. The upper image shows a circuit diagram of the bridge circuit. Middle images show translocation of a sample particle through the micropore. The lower graph shows the current signal due to translocation of a sample particle. (c) Photos of the micropore chip. The right image shows a micropore (red arrow) at the center of the micropore chip. Scale bars of left and right images are 1 cm and 25 μm , respectively.

Robust-ICS is possible in various environments and the analysis of detected bacteria is achieved with high accuracy.

EXPERIMENTAL SECTION

Fabrication of Bridge Circuit. The bridge circuit consisted of a micropore chip having a cross-channel structure and a micropore filled with a conductive solution, and two electric circuits, one for electrophoresis (red circuit in Figure 1 b) and one for ionic current sensing (blue circuit in Figure 1 b). In the electrophoresis circuit, the sample particle was electrophoresed by a voltage applied using a battery (6LR 61 YXJ/1 S, Panasonic) via an Ag wire (FTVS-408, Oyaide) and introduced into the micropore. In the ionic current sensing circuit, the potential difference at both ends of the 1 k Ω resistive element (E-Globalede Corp.) could be adjusted by operating the variable resistor (7270, BI Technologies). The current flowing through the amplifier (low noise current amplifier DLPCA-200, FEMTO) was output to a recorder composed of a signal converter (NI USB-6259, National Instruments) and a PC equipped with LabVIEW software (National Instruments). In ionic current sensing, the potential difference at both ends of the micropore and that of the 1 k Ω resistive element were used for the output signal. When there was no particle in the micropore, the circuit was adjusted to get a balanced state where no current flowed to the amplifier, resulting in the background current baseline becoming about 0 A (middle left image in Figure 1b). As the sample particle passed through the micropore, the potential difference at both ends of the micropore increased and the balance was lost; as a result, current flowed to the amplifier and was detected as a signal (middle center image and lower graph in Figure 1b). A high applied voltage gave a large current signal. In conventional methods, the applied voltage is generally several hundred millivolts to several volts because the background current baseline exceeds the detection upper limit when a high voltage is applied.⁸ In our past research, we created a balanced state to suppress the background

current and that allowed us to apply a high voltage to the circuit.¹⁸ The application of a high voltage enhanced the signal amplitude and compensated for the noise increase due to the simple electromagnetic shielding.

Fabrication of a Robust Ionic Current Sensor (Robust-ICS). We fabricated a robust ionic current sensor (Robust-ICS) by incorporating the bridge circuit into two boxes made of 1-mm-thick aluminum plates (Figure 2a). A microchip and Ag wires were installed

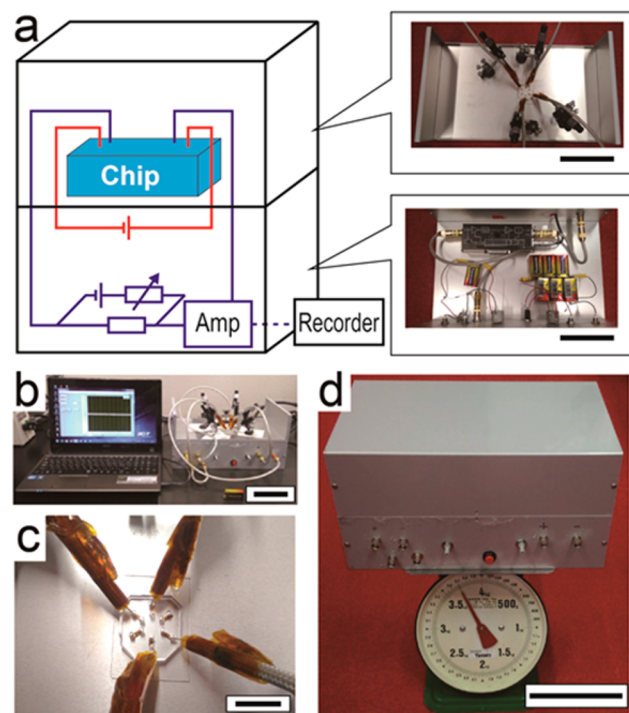


Figure 2. (a) Schematic illustration of Robust-ICS and photos of the two box interiors; scale bar, 15 cm. (b) Experimental setup of Robust-ICS; scale bar, 15 cm. (c) Photo of the micropore chip in Robust-ICS; scale bar, 2 cm. Ag wires were connected to reservoirs of the micropore chip. (d) Photo of Robust-ICS demonstrating its lightweight and compact size; scale bar, 15 cm.

in the upper box, and the two electric circuits for electrophoresis and ionic current sensing were placed in the lower box which was connected to a recorder (Figure 2b and c). By using a simple electromagnetic shield made of aluminum plates we lowered the weight of the two boxes to under 4 kg, and it became easier to carry the sensor device about and make detection measurements anywhere (Figure 2d).

Fabrication of the Micropore Chip. We made the micropore chip by pouring PDMS (SILPOT184, Dow Corning Toray Co., Ltd.) into a mold of SU-8 (SU-8 3005, Kayaku Co., Ltd.) formed by photolithography. In order to avoid contact between the sample solution and the wires when performing experiments using various samples consecutively, an Au electrode plate having a thickness of 40 nm was formed on a slide glass using a sputtering machine (MSP-mini, Vacuum Device), and a voltage was applied through the Au electrode plate (Figures 1c and S1). The micropore with a height of 3.7 μm , a width of 2.0 μm , and a length of 2.2 μm was fabricated at the center of the micropore chip. The micropore chip was filled with 5 \times TBE buffer (0.45 M Tris, 0.45 M boric acid, 0.01 M EDTA).

Scheme of Ionic Current Sensing for Particle Detection. A voltage of 50 V was applied to the micropore chip, and the variable resistor in the ionic current sensing circuit was operated to suppress the background current, which is the current value flowing to the ammeter, from 2 μA to under 10 pA. The solution containing the sample particles, such as polystyrene particles and bacteria, were dropped into the sample inlet. Since the particles were charged, they

could be introduced into the micropore by electrophoresis. The current signals obtained by passage of the sample particles through the micropore were measured.

We carried out an experiment to confirm the relationship between particle volume and signal amplitude using a commercially available shield box (Shield Room Corporation). The micropore chip and the two electric circuits were fixed in the commercial box, and the output current was measured outside the box. We carried out experiments for bacteria detection and noise measurement under various conditions using the robust-ICS with the aluminum plate boxes.

Sample Preparation. We evaluated performance of the bridge circuit using 0.50-, 0.75-, and 1.00- μm -diameter polystyrene particles (Fluoresbrite Calibration grade Microspheres) purchased from Polysciences, Inc. Volumes of 0.50-, 0.75-, and 1.00- μm -diameter polystyrene particles were 0.07, 0.22, and 0.52 fL, respectively. Polystyrene particles of each size were dispersed in $5 \times \text{TBE}$ buffer solution, and diluted to a concentration of 2×10^6 particles/mL for experiments. According to the product data sheet, 1.00 μm diameter particles have a standard deviation of 20 nm.

Staphylococcus aureus (ATCC 25923) and *Bacillus subtilis* (ATCC 6633) were cultured at 37 °C for 48 h using 2.5% LB medium (LB Broth miller, Sigma-Aldrich, Co.), washed with phosphate buffer (5 mM $\text{Na}_2\text{HPO}_4 \cdot 12\text{H}_2\text{O}$, 5 mM $\text{NaH}_2\text{PO}_4 \cdot 2\text{H}_2\text{O}$), and diluted to 10^6 cells/mL with $5 \times \text{TBE}$ buffer solution. For scanning electron microscope (Supra 40 VP, Carl Zeiss AG) observation, *S. aureus* cells were coated with a 10 nm thin layer of gold using the sputtering machine, and individual cell diameters were calculated using ImageJ software.

Ionic Current Sensing under Various Conditions. We confirmed the effects on ionic current sensing when using different electromagnetic shields, and when changing the temperature, humidity, and measurement place. The effect of different electromagnetic shields was confirmed by comparing the commercially available shield box which was made of 1 mm Galbarium steel and 26 mm aluminum plates and our box made of 1 mm aluminum plates for the Robust-ICS, in an experimental environment at a temperature of 25 °C and humidity of 20%. The effects of temperature and humidity changes were confirmed by placing the Robust-ICS, humidifier (Dew 054, Denkosha Co., Ltd.), and hot air blower (SU13-A, Tescom Co., Ltd.) in a plastic case (3-4055-21, AS ONE Corporation), and changing each condition (Figure S2). We calibrated the temperature and humidity in the plastic case by using a thermohygrometer (PC-7700SK, skSATO). The effect when changing the measurement place was examined by carrying out the ionic current sensing in four laboratories and outdoors. Laboratory 1 (Lab 1) had a size of 49 m², and a motorized microscope was an electromagnetic noise source. Laboratory 2 (Lab 2) had a size of 77 m², and two fume hoods, two refrigerators, a freezer, a deep freezer, and an ultrapure water preparation system were noise sources. Laboratory 3 (Lab 3) had a size of 24.5 m², and two fume hoods were noise sources. Laboratory 4 (Lab 4) had a size of 35 m², and two motorized microscopes were noise sources. Outdoor measurements were done on a grass area surrounded by buildings. A subway station was located within 30 m of the outdoor measurement place and the outdoor motor of an air conditioner unit was located within 10 m from the place.

RESULTS AND DISCUSSION

Relationship between Sample Particle Volume and Signal Amplitude. In this paper, we defined the difference between the background current baseline and the lowest current value in a passing sample particle as the signal amplitude (Figure 3). Comparison of the signal amplitudes of 0.50-, 0.75-, and 1.00- μm -diameter polystyrene particles indicated the volume of the sample and the signal amplitude had a proportional relationship. The signal amplitudes of 0.50-, 0.75-, and 1.00- μm -diameter polystyrene particles were 1.16 nA, 4.96 nA, and 10.2 nA, respectively. This result is consistent with the detection principle that particles with larger volume

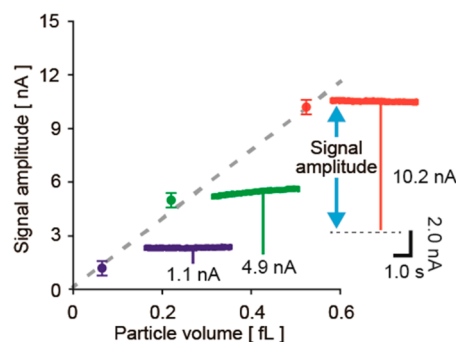


Figure 3. Signal amplitude of 0.50-, 0.75-, and 1.00- μm -diameter polystyrene particles. Each point shows the average signal amplitude of 0.50-, 0.75-, and 1.00- μm -diameter polystyrene particles. The gray dotted line is an approximation curve of the relationship between particle volume and signal amplitude. Blue, green, and red lines are current signals of 0.50-, 0.75-, and 1.00- μm -diameter polystyrene particles. Error bars show the standard deviation for a series of measurements ($N = 200$).

decrease the current value by eliminating more conductive solution in the micropore. Therefore, the sample diameter can be calculated from the signal amplitude. Particle size detection based on the signal amplitude shows high repeatability (Figure S3).

Application to Bacteria Detection. As an application for bacterial detection, *S. aureus* was detected with our Robust-ICS and the calculated cell diameter was compared with the result obtained by SEM observation (Figure 4). *S. aureus* is one of the bacteria harmful to the human body and has a diameter size of 1 μm or less¹⁹ (Figure 4a). Using Robust-ICS, we detected 200 cells in 115 s, and the cell diameter was calculated from the signal amplitude (Figure 4b). The histogram of cell diameters

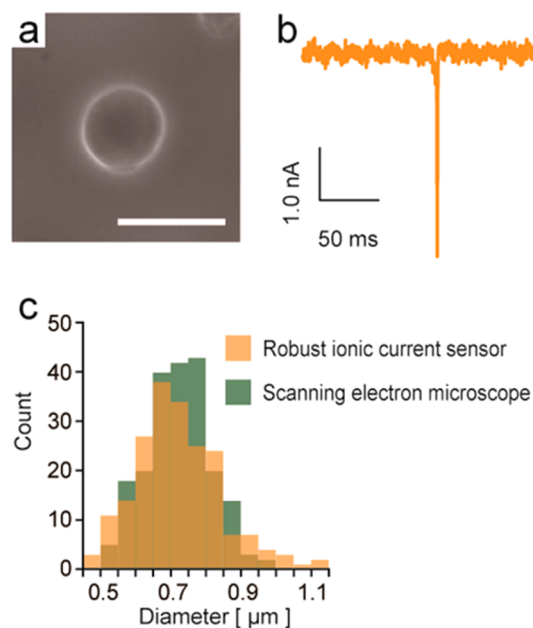


Figure 4. Detection of bacteria by using Robust-ICS. (a) SEM image of *S. aureus*; scale bar, 1 μm . (b) Current signal of an individual *S. aureus* cell. (c) Comparison histogram of the detected diameter of *S. aureus* cells obtained using SEM and Robust-ICS. The number of measured cells in both experiments was 200. Detection time for 200 cells using Robust-ICS was 115 s.

measured using SEM corresponded to that of cell diameters detected using the Robust-ICS (Figure 4c). The average value of the cell diameter in both observations was $0.72 \mu\text{m}$. There was no significant difference in the average value ($p\text{-value} = 0.92 > 0.05$). Detected volumes of *S. aureus* and *B. subtilis* were clearly different (Figure S4). Therefore, Robust-ICS can accurately detect the particle size of biological samples, and size-based bacteria discrimination is realized.

Effect of the Measurement Environment. Using the amplitudes of current noise in ionic current sensing as an indicator, we confirmed the effect of the experimental environment on ionic current sensing (Figure 5a). The

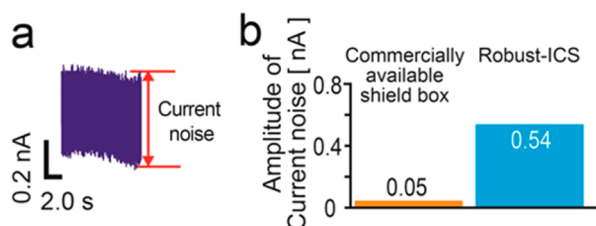


Figure 5. Comparison of the amplitude of current noise in ionic current sensing in two shield boxes with different shielding performances. (a) Definition of current noise in this paper. Amplitude of current noise was the average value of 10 s measurement. (b) Difference in amplitude of current noise by changing the electromagnetic shield.

amplitude of current noise in ionic current sensing with Robust-ICS was ten times larger than that in ionic current sensing with the commercially available shield box (Figure 5b). Due to the difference in the shielding performance of the box materials and the box air tightness, Robust-ICS, which has the simple electromagnetic shield, showed larger amplitudes of current noise. Because the commercially available shield box weighed over 50 kg, it had low portability; hence shielding performance and portability were in a trade-off relationship. The amplitude of current noise of Robust-ICS was 0.54 nA , which is enough to detect submicron size particles such as $0.5 \mu\text{m}$ particles by using the bridge circuit.

Comparing the current noise in current sensing at room temperature and high temperature while changing humidity in the plastic case, we found the amplitude of the current noise was constant in all situations (Figure 6). Since average amplitudes of current noise were 0.43 nA at 25 to $27 \text{ }^\circ\text{C}$ and 0.43 nA at 37 to $40 \text{ }^\circ\text{C}$, thermal noise from the temperature was not the main factor determining the amplitudes of current noise in Robust-ICS. Similarly, there was no difference in amplitudes

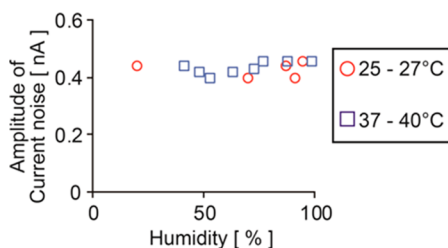


Figure 6. Comparison of the amplitude of current noise in ionic current sensing at various temperature and humidity conditions. At 25 to $27 \text{ }^\circ\text{C}$, measurements were done at humidities of 20%, 70%, 87%, 91%, and 95%. At 37 to $40 \text{ }^\circ\text{C}$, measurements were done at humidities of 41%, 48%, 53%, 63%, 73%, 77%, 88%, and 99%.

of current noise between humidities of 20% and 99%. Based on these results, Robust-ICS can measure samples with the same detection limit under any temperature and humidity conditions except when a short circuit is caused by water condensation.

When measurements were performed in the four laboratories of different sizes and having different electromagnetic noise sources, a difference in the amplitude of the current noise of 200 pA in current sensing was observed (Figure 7a). No

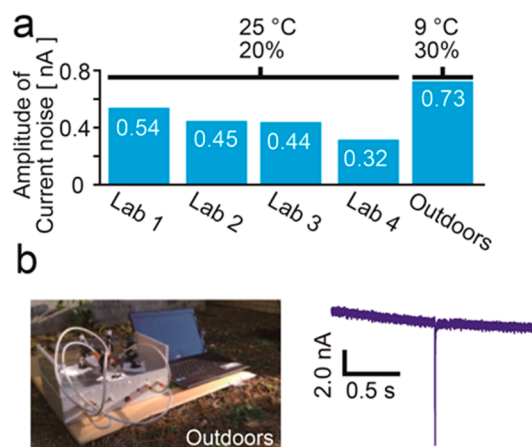


Figure 7. Comparison of amplitude of current noise at various places and detection of $1 \mu\text{m}$ particles outdoors. (a) Comparison of noise at various places. (b) Detection of $1 \mu\text{m}$ polystyrene particles done outdoors. Left image shows the experimental setup outdoors. Right graph shows the current signal of an individual $1\text{-}\mu\text{m}$ -diameter polystyrene particle obtained outdoors.

correlation was found between the difference in types and numbers of noise source devices in the laboratories and the amplitudes of current noise. Even in Lab 1 which had the largest amplitudes of current noise among the four laboratories, detection of submicron particles such as $0.5 \mu\text{m}$ particles was possible. In the outdoor measurements, the amplitude of current noise was much larger. We considered that the electromagnetic noise from the surroundings (the subway station and the air conditioner motor) and the vibration derived from the wind influenced the amplitudes of current noise in ionic current sensing. Without using a vibration removal board, Robust-ICS kept a constant amplitude of current noise which was enough to detect submicron particles larger than $0.5 \mu\text{m}$. A polystyrene particle of $1 \mu\text{m}$ in diameter was successfully detected by Robust-ICS outdoors (Figure 7b). The obtained signal amplitude was 10.72 nA and the calculated particle diameter was $1.01 \mu\text{m}$; therefore, the signal amplitude corresponded to the reference value in the product data sheet.

Although Robust-ICS has low shielding performance and it is affected by surrounding electromagnetic noise sources, particles over $0.5 \mu\text{m}$ in diameter can be detected because the amplitude of the current noise is always lower than 1 nA . A lower detection limit can be obtained by decreasing the amplitude of the current noise and enhancing the current signals. The amplitude of current noise can be decreased by increasing air tightness of the shielding aluminum box. Signals can be enhanced by increasing the applied voltage and the concentration of conductive solution in the micropore chip. Compared with conventional ionic current sensing methods, our Robust-ICS using the bridge circuit can tolerate a large current flow because the background current is suppressed.

Even at the present performance levels of Robust-ICS, *S. aureus* with a diameter of about 1 μm , can be detected anywhere.

CONCLUSIONS

We succeeded in obtaining a high S/N ratio by fabricating a robust ionic current sensor (Robust-ICS) using a bridge circuit, and as a result, we successfully detected bacteria even in a large noise condition using just a simple, lightweight electromagnetic shield made of aluminum plates. The weight of our Robust-ICS was under 4 kg. The calculated diameter of bacterial cells detected by Robust-ICS was consistent with the result by SEM imaging. When temperature, humidity, and measurement places were changed, the amplitude of current noise in ionic current sensing was smaller than 1.0 nA and it did not affect detection of particles over 0.5 μm in diameter. Even large size bacteria and clusters of small bacteria can be detected with the same micropore if its cross-sectional area is not larger than that of the micropore. The diameter of 1 μm particles was accurately detected in outdoor measurements. Although same-sized bacteria species cannot be discriminated by ionic current sensing, integration of a microscope,²⁰ which can observe a cell surface, into Robust-ICS should enable discrimination based on the size and cell surface property of the bacteria. In addition, discrimination of bacteria based on cell shapes can be done by using a low-aspect-ratio micropore.²¹ On-site inspection using Robust-ICS will make it easier to determine bacteria on the surface of equipment or in such samples as foods and body fluids of patients.

ASSOCIATED CONTENT

Supporting Information

The Supporting Information is available free of charge on the ACS Publications website at DOI: 10.1021/acssens.8b00045.

Micropore chip fabrication process, and experimental setup to get various temperature and humidity conditions (PDF)

AUTHOR INFORMATION

Corresponding Authors

*E-mail: yasaki.hirotooshi@e.mbox.nagoya-u.ac.jp.

*E-mail: babaymtt@apchem.nagoya-u.ac.jp.

ORCID

Hirotooshi Yasaki: 0000-0001-6985-9073

Takao Yasui: 0000-0003-0333-3559

Takeshi Yanagida: 0000-0003-4837-5701

Author Contributions

H. Y., T. S., T. Yasui, T. Yanagida, N. K., M. K., K. N., T. K., and Y. B. planned and designed the experiments. H. Y. and T. S. performed experiments. H. Y., T. Yasui, T. Yanagida, N. K., M. K., and K. N. analyzed data. H. Y., T. S., T. Yasui, T. Yanagida, N. K., M. K., and K. N. wrote the paper.

Notes

The authors declare no competing financial interest.

ACKNOWLEDGMENTS

This research was supported by Grants-in-Aid for JSPS Research Fellow (15J03490, 17J05751), PREST (JPMJPR151B, JPMJPR16F4), JST, the JSPS Grant-in-Aid for Young Scientists (A) 17H04803, the ImpACT Program of the Council for Science, Technology and Innovation (Cabinet

Office, Government of Japan), and the JSPS Grant-in-Aid for Scientific Research (A) 16H02091.

REFERENCES

- (1) Le Loir, Y.; Baron, F.; Gautier, M. Staphylococcus aureus and food poisoning. *Genet. Mol. Res.* **2003**, *2*, 63–76.
- (2) Hauge, S. Food poisoning caused by aerobic spore-forming bacilli. *J. Appl. Bacteriol.* **1955**, *18*, 591–595.
- (3) Evenson, M. L.; Hinds, M. W.; Bernstein, R. S.; Bergdoll, M. S. Estimation of human dose of staphylococcal enterotoxin A from a large outbreak of staphylococcal food poisoning involving chocolate milk. *Int. J. Food Microbiol.* **1988**, *7*, 311–316.
- (4) Ostyn, A.; De Buyser, M.; Guillier, F.; Groult, J.; Felix, B.; Salah, S.; Delmas, G.; Hennekinne, J. First evidence of a food poisoning outbreak due to staphylococcal enterotoxin type E, France, 2009. *Euro Surveill.* **2010**, *15*, 1–4.
- (5) Sethi, S.; Murphy, T. F. Bacterial infection in chronic obstructive pulmonary disease in 2000: a state-of-the-art review. *Clin. Microbiol. Rev.* **2001**, *14*, 336–363.
- (6) Lowy, F. D. Staphylococcus aureus infections. *N. Engl. J. Med.* **1998**, *339*, 520–532.
- (7) Wieneke, A.; Roberts, D.; Gilbert, R. Staphylococcal food poisoning in the United Kingdom, 1969–90. *Epidemiol. Infect.* **1993**, *110*, 519–531.
- (8) Bayley, H.; Martin, C. R. Resistive-Pulse Sensing-From Microbes to Molecules. *Chem. Rev.* **2000**, *100*, 2575–2594.
- (9) Gregg, E. C.; Steidley, K. D. Electrical counting and sizing of mammalian cells in suspension. *Biophys. J.* **1965**, *5*, 393–405.
- (10) Yu, A. C. S.; Loo, J. F. C.; Yu, S.; Kong, S. K.; Chan, T. F. Monitoring bacterial growth using tunable resistive pulse sensing with a pore-based technique. *Appl. Microbiol. Biotechnol.* **2014**, *98*, 855–862.
- (11) Henriques, A. O.; Glaser, P.; Piggot, P. J.; Moran, C. P., Jr. Control of cell shape and elongation by the rodA gene in *Bacillus subtilis*. *Mol. Microbiol.* **1998**, *28*, 235–247.
- (12) Song, H.; Wang, Y.; Rosano, J. M.; Prabhakarandian, B.; Garson, C.; Pant, K.; Lai, E. A microfluidic impedance flow cytometer for identification of differentiation state of stem cells. *Lab Chip* **2013**, *13*, 2300–2310.
- (13) Asghar, W.; Wan, Y.; Ilyas, A.; Bachoo, R.; Kim, Y. T.; Iqbal, S. M. Electrical fingerprinting, 3D profiling and detection of tumor cells with solid-state micropores. *Lab Chip* **2012**, *12*, 2345–2352.
- (14) Garza-Licudine, E.; Deo, D.; Yu, S.; Uz-Zaman, A.; Dunbar, W. B. In *Engineering in Medicine and Biology Society (EMBC), 2010 Annual International Conference of the IEEE; IEEE*, 2010; pp 5736–5739.
- (15) Ilyas, A.; Asghar, W.; Ahmed, S.; Lotan, Y.; Hsieh, J.-T.; Kim, Y.-t.; Iqbal, S. M. Electrophysiological analysis of biopsy samples using elasticity as an inherent cell marker for cancer detection. *Anal. Methods* **2014**, *6*, 7166–7174.
- (16) Particle Technology Laboratories <http://www.particletechlabs.com/>; (Accessed November 10, 2017).
- (17) Garza-Licudine, E.; Deo, D.; Yu, S.; Uz-Zaman, A.; Dunbar, W. B. Portable Nanoparticle Quantization using a Resizable Nanopore Instrument - The IZON qNano (TM). *Ieee Eng. Med. Bio* **2010**, 5736–5739.
- (18) Yasaki, H.; Yasui, T.; Yanagida, T.; Kaji, N.; Kanai, M.; Nagashima, K.; Kawai, T.; Baba, Y. Substantial Expansion of Detectable Size Range in Ionic Current Sensing through Pores by Using a Microfluidic Bridge Circuit. *J. Am. Chem. Soc.* **2017**, *139*, 14137–14142.
- (19) Foster, T. *Medical Microbiology Chapter 12*, 4th ed.; Univ of Texas Medical Branch: Galveston, 1996.
- (20) Yasaki, H.; Yasui, T.; Rahong, S.; Yanagida, T.; Kaji, N.; Kanai, M.; Nagashima, K.; Kawai, T.; Baba, Y. Micropore channel-based simultaneous electrical and optical sensing from biomolecules, single exosomes to single cells. *Proc. μ TAS2014* **2014**, *1*, 2161–2163.
- (21) Tsutsui, M.; Yoshida, T.; Yokota, K.; Yasaki, H.; Yasui, T.; Arima, A.; Tonomura, W.; Nagashima, K.; Yanagida, T.; Kaji, N.; Taniguchi, M.; Washio, T.; Baba, Y.; Kawai, T. Discriminating single-

bacterial shape using low-aspect-ratio pores. *Sci. Rep.* **2017**, *7*, 17371–17379.